Macromolecules

ARTICLE

pubs.acs.org/Macromolecules

Template-Free Deposition of Polyaniline Nanostructures on Solid Substrates with Horizontal Orientation

Chuanjun Liu,* Kenshi Hayashi, and Kiyoshi Toko

Department of Electronics, Graduate School of Information Science and Electrical Engineering, Kyushu University, 744, Motooka, Nishiku, Fukuoka 819-0395, Japan

ABSTRACT: By investigating the electrochemical nucleation and growth of polyaniline (PANI) on the insulating gap area of an interdigitated electrode, a template-free, in-situ approach is developed to obtain PANI nanowires and nanofibers with horizontal orientation on solid substrates. Experimental results show that the deposition process of PANI on the gap area is significantly influenced by polymerization conditions (such as polymerization current and time) and surface characteristics of the substrates (such as hydrophilicity/hydrophobicity and roughness). The concentration of solution-formed oligomers and the nucleation amount of the oligomers on the solid surface determine the morphology and orientation of the nanostructures. Controlling the deposition with high oligomer concentrations and limited nucleation amounts on the substrate is the key to the horizontal orientation. Gas sensing experiments confirm that the horizontal orientation of the nanostructures helps to improve the sensitivity and response time of sensor devices. Because of its simplicity, the approach proposed in this paper can be used in the fabrication of nanostructured conducting polymer chemiresistive gas sensor with high sensitivity but low cost.

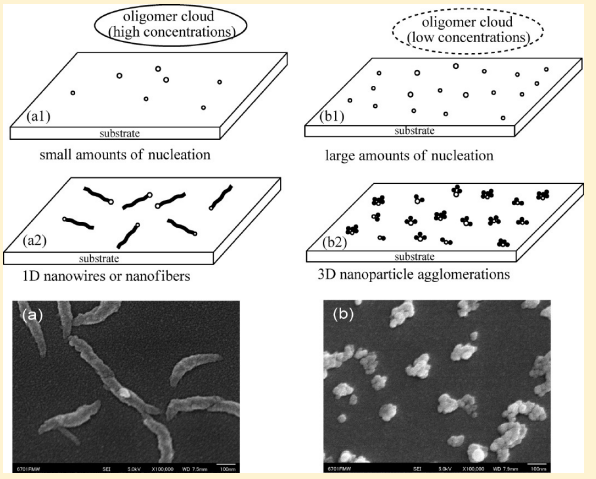

INTRODUCTION

The application of conducting polymers (CPs) with one-dimensional (1D) nanostructures (such as nanowires and nanofibers) to fabricate organic electrical devices has attracted considerable attention owing to their reduced dimensionality, high aspect ratio, and unique electron transport properties.[1−6] Enhancing the orientation of the nanostructures has been proved to be an effective method to improve the performance of the fabricated devices.[7] Generally, there are two basic types of orientations: perpendicular and horizontal to the substrate surface. Up to now, the perpendicular orientation of nano-CPs has been realized successfully by both template-based and template-free polymerization (chemical oxidation or electrochemical deposition) on conducting or nonconducting substrates.[7−12] The perpendicular orientation is advantageous for the nanostructures to be applied as electrochemical or biological sensors in view of a highly effective surface area and a fast diffusion kinetics. However, for some special applications, such as chemiresistive gas or organic vapor sensors, the horizontal orientation of the nanostructures is desirable because the change of resistance is measured in the direction parallel to the substrates. Comparatively, little attention has been paid on the template-free preparation of CP nanostructures oriented horizontally with respect to solid substrates.

The most common nano-CP chemiresistive sensors are fabricated by drop-casting a suspension of presynthesized polyaniline (PANI) nanofibers on interdigitated electrodes.[13]The lack of alignment in the nanofibers is an inadequacy of this method, although the sensors give better performance in both sensitivity and response time than conventional PANI films. Electrochemical growth of CP films (including polyaniline, polypyrrole, and polythiophene, etc.) by lateral spreading cross a gap electrode to form resistive junctions is another representative method which has long been used to fabricate organic vapor sensors.[14,15] Unfortunately, the lateral spreading affords only a compact film rather than nanostructures on the insulating gap area. By use of a well-known stepwise electrochemical polymerization, a CP nanoframework can be formed to bridge the electrodes with a gap width of several micrometers.[16−18] The misalignment and overlapping of the nanostructures are still problems that need to be improved. Additionally, it has been suggested in those works that the formation of the nanoframework originates from the deposition of PANI nanowires on the working electrodes and the subsequent propagation of the nanowires across the electrode gaps. However, the latest reports on the electrochemical growth mechanism of CPs have demonstrated that a 2D compact film is very likely to be deposited on the gap area prior to the formation of the top layer nanoframework. Thus, special surface treatments are needed to prevent the "unwanted" formation of the bottom compact layer on silicon-based substrates.[19,20] Recently, the

Received: October 20, 2010
Revised: December 21, 2010
Published: March 02, 2011

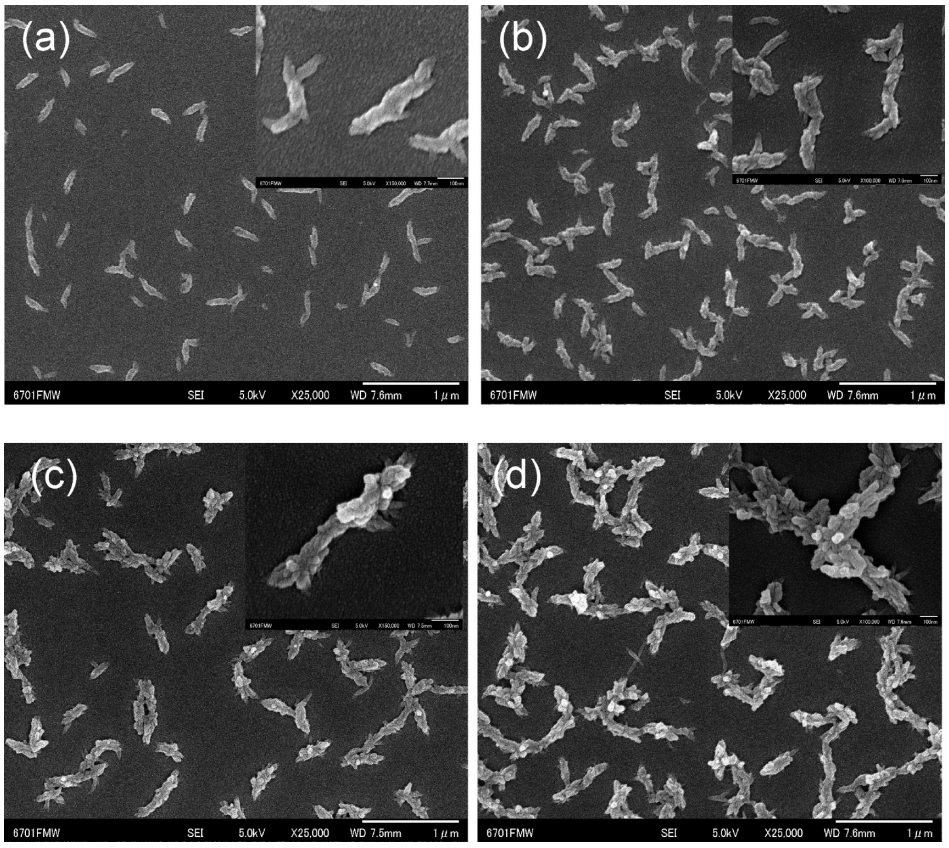

Figure 1. SEM images of PANI deposited on the insulating gap area of a glass-based interdigitated electrode with high hydrophilicity. The polymerization current is 1 μA, and the polymerization time is 1800 (a), 2700 (b), 3600 (c), and 4500 s (d). The insets are the images with high magnification.

preparation of individually addressable single (or multiple) nanowire devices with highly controlled dimension and orientation has also been reported by electrochemical growth between nano- or microscaled gap electrodes to form resistive junctions.[21−24] This technique shows great advantages in the integration of oriented nanomaterials with nanoscale devices. However, because of highly technical requirements for the preparation of prepatterned nanogap or nanochannel electrodes, the application of this method in the present stage is limited by problems such as yield, reproducibility, and most of all cost.

In this study, we report a simple and template-free electrochemical approach to obtain PANI nanowires and nanofibers with the horizontal orientation on the insulating gap area of an interdigitated electrode. The electrodes used have gap widths ranging from tens of micrometers to 100 μm, which can be facilely prepared by standard photolithography technique on Au-deposited glass substrates. The electrochemical polymerization is performed galvanostatically in a classic three-electrode cell, in which the comb-shaped Au electrode pairs are shorted as the working electrode. The influence of polymerization conditions (polymerization current and time) and surface characteristics (hydrophilicity/hydrophobicity and roughness) on the morphology of the deposited PANI is investigated. A mechanism for the formation of PANI with different nanostructures and orientations under different polymerization conditions is proposed. Gas sensing experiments are carried out to confirm that the horizontal orientation helps to improve the sensing performance of the fabricated chemiresistive sensors.

EXPERIMENTAL SECTION

Electrodes. The interdigitated electrodes used in this work were fabricated by standard photolithography technique using a gold/glass plate (200 nm Au/20 nm Ti on Corning Eagle XG glass obtained from IDEA System Co., Ltd., Japan). The electrode geometry consists of five pairs of gold fingers, each finger having dimensions of 100 μm × 2200 μm × 0.2 μm (width × length × height). The gap width between neighboring fingers is typically 100 μm, but the same experimental results can be observed for other electrodes with much narrower gap widths (for example, 10 μm).

Surface Treatment. The electrodes with a highly hydrophilic character (contact angle is lower than 5°) on the insulating gap area were obtained by cleaning them for 1 h using piranha solution (98% H_2SO_4:30% H_2O_2 at 7:3 v/v) that was preheated to 100 °C. *CAUTION: piranha reacts violently with organic solvents, and should be handled with extreme caution.* Two kinds of alkylsilane reagents, 3-aminopropyltriethoxysilane (APTES) and octyltriethyoxysilane (OTES) (Shinetsu Chemical Industries, Ltd., Japan), were used to adjust the hydrophilic/hydrophobic character of the insulting gap areas. The electrodes were first treated with argon plasma, followed by immerging in a 3% toluene solution of APTES for 6 h or OTES for 3 h. Then, they were rinsed with pure toluene three times. The APTES-treated electrodes were cured in an air permeable but dust-free container for 24 h and incubation in deionized Millipore water for another 24 h.

Electrochemical Polymerization. The electrochemical polymerization was carried out by using an Autolab PGSTAT302 potentiostat/galvanostat. The comb-shaped gold electrodes were masked with an effective working area of 0.07 cm^2. A Pt coil served as the counter

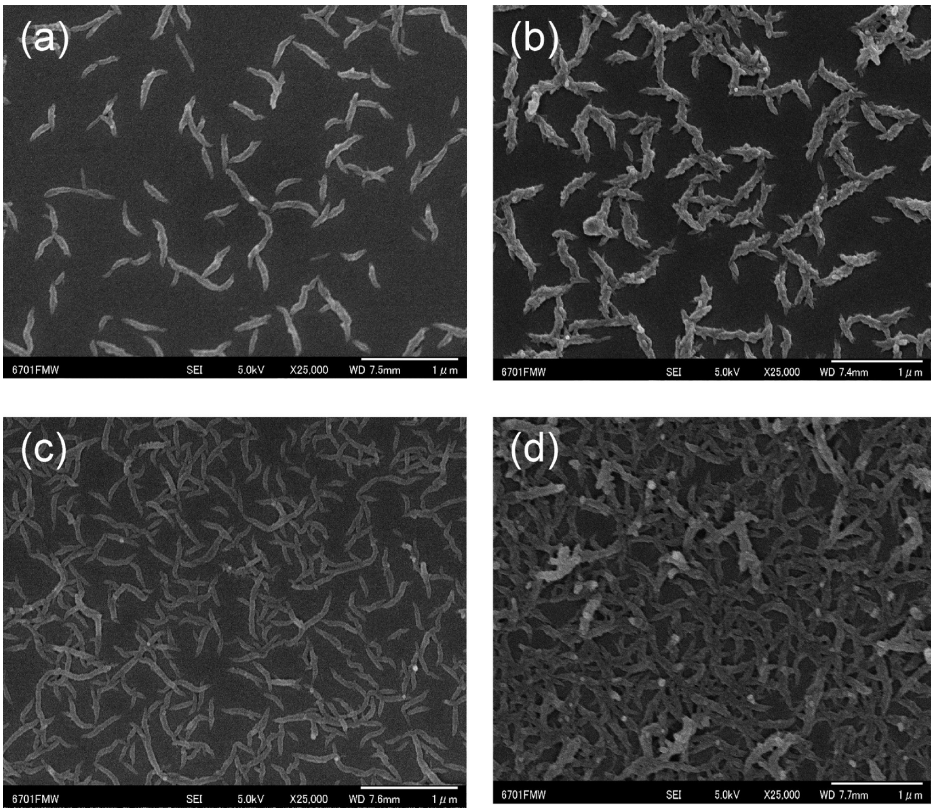

Figure 2. SEM images of PANI deposited on the gap area of the hydrophilic electrodes with increased polymerization currents: (a) 3 μA/1800 s, (b) 3 μA/2700 s, (c) 6 μA/900 s, (d) 6 μA/1800 s.

electrode, and a standard Ag/AgCl functioned as the reference electrode. The electrodes were immerged in an electrolyte solution consisting of 0.05 M aniline and 1.0 M HCl. Constant currents were applied to deposit PANI films on the insulating gap area with different nanostructures.

Characterization. The morphology of the prepared PANI film on the gap area of the interdigitated electrodes was investigated with a field-emission scanning electron microscope (FESEM, JSM-6701F; JEOL, Japan) at the Center of Advanced Instrumental Analysis, Kyushu University.

Ammonia Gas Sensing. An ammonia permeation tube (P-3, GASTEC Co., Japan) set in a standard gas generator (PERMEATOR PD-1B, GASTEC Co., Japan) was used to generate NH_3 gas with a standard concentration of 1 ppm. A homemade multisensing system, equipped with a LCR meter (ZM2371, NF Corp., Japan) and a custom LabView computer program, was used to record the impedance variation of the PANI electrodes upon exposure to NH_3 gas flow.

RESULTS AND DISCUSSION

It is generally considered that a hydrophilic surface is not favorable for the deposition of CPs due to the hydrophobic character of monomer and oligomer intermediates.[19,25,26] However, we find that the deposition of PANI on the insulating gap area is almost unavoidable during the electrochemical process even if the glass-based interdigitated electrodes are cleaned with hot piranha solution (or plasma cleaning) and show a superhydrophilic character with a contact angle close to zero. Additionally, different from the uniform film or granular particulate structure as conventionally observed in the in-situ chemical deposition or coating of PANI on solid substrates,[27−32] the SEM image in Figure 1a indicates that PANI nanowires are deposited on the gap area when the polymerization is carried out with a current of 1 μA and a time of 30 min. The diameters of the nanowires are less than 80 nm, and the lengths can prolong to several hundreds of nanometers (Figure 1b). All of the nanowires are lodged in the surface, indicating that the growth direction in the initial polymerization is oriented horizontally to the substrate. With the increasing in polymerization time, the 1D growth character seems to be changed because agglomeration of globular nanoparticles on the previously formed nanowires is observed (Figure 1c). The agglomeration results in the concurrent thickening and lengthening but with the rate of lengthening faster than that of thickening. Simultaneously, it is observed that the agglomeration provides nucleation sites to form branched nanofiber network in the later stage of the polymerization. During the whole polymerization, the nanowires or nanofibers are homogeneously dispersed on the gap area, and no difference in the deposition density is observed between the area near the Au working electrode and the middle area of the gaps.

Recent studies on the synthesis of nano-CPs have revealed that the key point in producing 1D nanostructures is to promote the homogeneous nucleation (i.e., primary growth), which generally results in an inherent nanofiber structure, or to suppress the heterogeneous nucleation (i.e., the secondary growth), which generally results in an agglomerated morphology.[11,33,34] This concept has been widely used in the template-free chemical oxidative or electrochemical polymerization of CP nanowires and nanofibers. It is worth noting that the 1D character of PANI as shown in Figure 1a indicates that the deposition in the initial stage is dominated by the homogeneous nucleation process, which disobeys the heterogeneous nucleation process that generally occurs on the solid−solution interface.[35,36] Apparently, the homogeneous nucleation and growth in the initial polymerization are of special interest because they tends

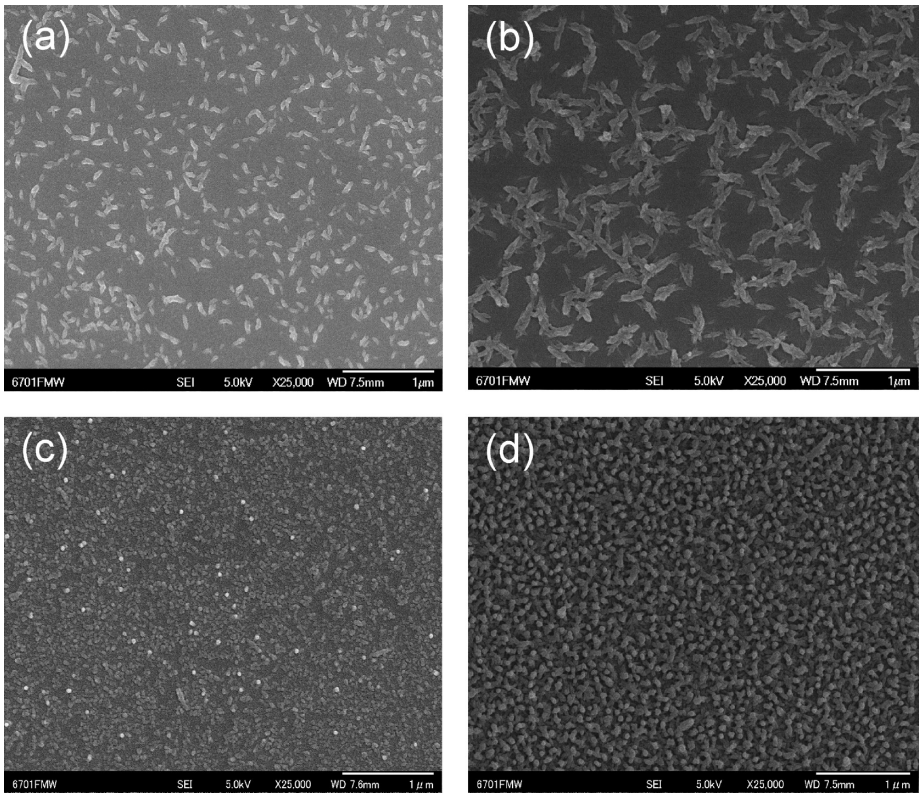

Figure 3. SEM images of PANI deposited on the insulating gap area treated by silane reagents: (a) APTES-treated, 1 μA/1800 s; (b) APTES-treated, 1 μA/3600 s; (c) OTES-treated, 1 μA/1800 s; (d) OTES-treated, 1 μA/3600 s.

to give the nanostructures oriented horizontally to the substrate surface. According to the classic nucleation theory,[37] the precondition for the occurrence of the homogeneous nucleation is to create a sufficiently high level of supersaturation. In the polymerization as shown in Figure 1, we think that various factors, such as the low aniline concentration (50 mM), the low polymerization current (1 μA), the hydrophilic surface, and even the electrode geometry, might contribute to form the supersaturation state of oligomers on the insulating gap area. The low monomer concentration and the low polymerization current lead to a slow nucleation and growth process of solution-formed oligomers on the Au working electrodes. Some parts of the oligomers diffuse away and form an oligomer cloud on the insulating gap area. Owning to the high interfacial energy caused by the highly hydrophilic character of the substrate, the oligomers are hard to nucleate on the surface of the gap area in the initial stage. This results in a continuous increase in oligomer concentration. Therefore, the homogeneous nucleation occurs in the solution phase. Once the oligomer nuclei exceed a critical size, they precipitate from the solution and deposit on the gap area. Subsequently, the homogeneous nucleation and anisotropic growth continue to occur on the deposited nuclei, which afford the observed nanowire structure. With the development of polymerization, especially after the Au working electrode is completely covered by a thin film of PANI, the polymerization on the Au working electrode area should be accelerated because the oxidative potential of aniline on the PANI film is lower than that on the bare Au electrodes.[38] As a result, the supersaturation state on the gap area is destroyed in view of the insufficient diffusion of oligomers. At the same time, the formerly deposited nanowires can act as the heterogeneous nucleation sites for the ensuing growth of PANI. Thus, the agglomeration of globular nanoparticles on the formerly formed nanowires is observed, which results in the branched structure as shown in Figure 1d.

In order to get an extensive understanding on the deposition mechanism, the morphology of PANI deposited on the insulating gap area under different polymerization conditions was investigated. First, the polymerizations were carried out on the piranha solution-cleaned interdigitated electrodes with increased currents. As shown in Figure 2a, the morphology of deposited PANI changes dramatically from short nanowires to long nanofibers. Compared with the result shown in Figure 1a, the increase in polymerization current to 3 μA seems to have no obvious influence on the diameter of the nanostructures and the number of nucleation sites on the gap area. The only effect observed is the increase in the length of nanostructures in the 1D direction. When the polymerization current is further increased to 6 μA, the well-developed nanofibers are obtained in a much shorter time (see Figure 2b). However, the branching and disorientation become obvious as well, which can be attributed to the accelerated heterogeneous nucleation and growth under high polymerization currents. The results shown in Figure 2 confirm that the high oligomer concentration, i.e., supersaturation sate, plays an important role in the formation of 1D nanostructure as discussed according to the classic nucleation theory.

The polymerizations were also carried out on the interdigitated electrodes pretreated with different silane reagents. Two kinds of reagents, 3-aminopropyltriethoxysilane (APTES) and octyltriethyoxysilane (OTES), were used to modify the hydrophilic/hydrophobic character of the insulating gap area. The average contact angles measured for APTES- and OTES-treated glass substrates were 20° and 90°, respectively. The SEM images shown in Figure 3a indicate that under the same polymerization

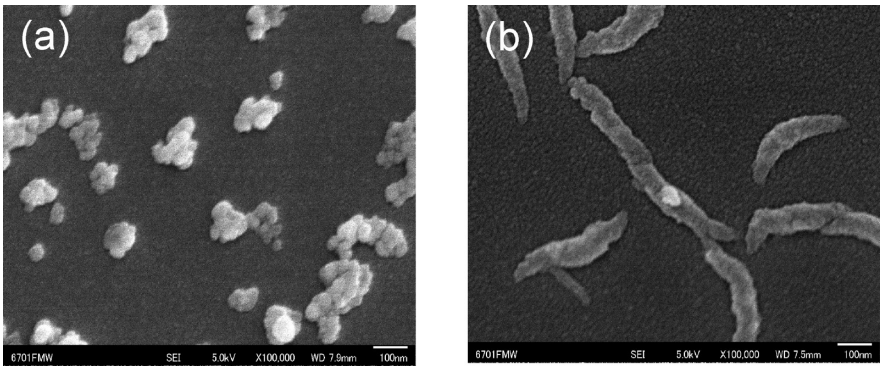

Figure 4. (a) SEM image of PANI nanoparticle agglomeration structure deposited on the Au-NPs treated electrodes (1 μA/450 s). (b) SEM image of PANI nanofiber structure deposited on the bare hydrophilic electrodes (3 μA/1800 s).

condition a small increase in contact angle results in a great increase in the amount of nucleation sites. At the same time, the nanowire structure shown in Figure 1a is changed to a much shorter nanorod structure. For the deposition on the OTES-treated, hydrophobic surface (Figure 3b), the gap area is rapidly covered by a thin mat composed by dense nanonodules. The ensuing growth of PANI nanowires on these nodules shows a character of perpendicular orientation, which is similar to the template-free electrochemical deposition that occurs on conducting substrates.[7,11] It is not surprising that the nucleation amount increases with the increase in the contact angle because the hydrophobic surface tends to reduce the interfacial energy between the substrate and the oligomer nuclei. Apparently, large amounts of nucleation on hydrophobic surfaces are not favorable for the growth of 1D nanostructures, not to mention the horizontal orientation. The above results can be used to explain why horizontally oriented nanostructures have never been reported as yet on hydrophobic substrates, such as plastics, resins, and metals, no matter by chemical oxidative polymerization or electrochemical polymerizations.

Additionally, we noticed that the surface roughness also had significant influence on the morphology of deposited PANI, as reported by our previous work.[39] When a layer of gold nanoparticles (Au-NPs) is ion-sputtered on the bare electrodes to increase the surface roughness of the gap area,[39,40] the polymerization in the initial stage results in a structure comprised of agglomerated nanoparticles (see Figure 4a), which is completely different from the nanofiber structure as shown in Figure 4b (the high magnification image of Figure 2a-1). In order to figure out the reason why these two kinds of extreme structures are formed by the different deposition processes, the chronopentiogram of polymerizations carried out under different conditions was investigated. As shown in Figure 5, in comparison to the polymerization on the Au-NPs treated electrodes (curve a), a potential disturbance is observed on the bare electrodes (curves b and c), which is characterized by the appearance of a shoulder peak before the potential reaches its maximum. This potential disturbance effect is particularly obvious for curve b, which is corresponding to the nanofiber structures prepared with a high polymerization current on the hydrophilic electrode. We suggest that the appearance of the potential shoulder peak is caused by a transient decrease of polymerization efficiency due to the oligomer diffusion in the initial polymerization. Although this diffusion process occurs similarly on the Au-NPs deposited electrodes, the potential disturbance is suppressed greatly by the fast nucleation and growth of PANI both on the Au working electrodes

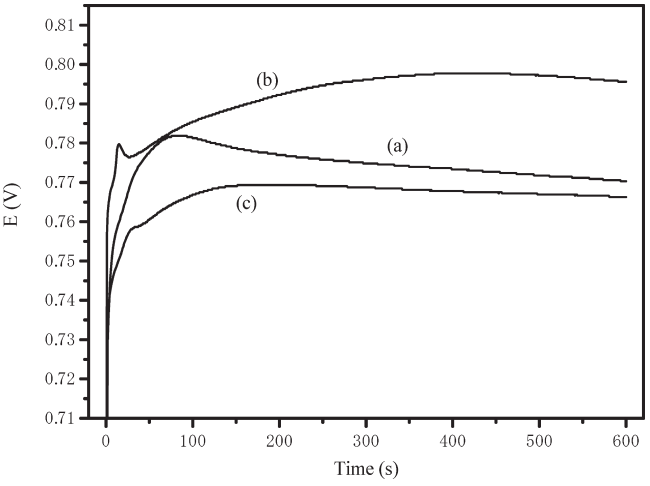

Figure 5. Chronopotentiograms of polymerization with different conditions. Curves a, b, and c are corresponding to the polymerizations as shown in Figure 4a (Au-NPs treated electrode, 1 μA), Figure 4b (bare hydrophilic electrode, 3 μA), and Figure 1a (bare hydrophilic electrode, 1 μA), respectively.

and the insulating gap area. In our previous work, this phenomenon was attributed to the inductive effect caused by the increase in surface roughness.[39]

Another obvious difference between curves a and b in Figure 5 is the time to reach the potential maximum (T_{max}). In the case of curve a the T_{max} is about 80 s, while in the case of curve b the T_{max} is extended to about 400 s. It has been suggested that the T_{max} is associated with the time needed for the Au working electrode to be covered by the formation of a thin PANI film.[41,42] A longer T_{max} is corresponding to a slower deposition of oligomers on the working electrode, in which more oligomers can diffuse to the gap area to maintain the supersaturation state. In the case of curve a, the fast deposition results in a low oligomer concentration but a large amount of nucleation on the insulating gap area. This is exactly a favorable environment for the heterogeneous nucleation. As a result, the oligomers are deposited in the form of nanoparticle agglomerations. It should be mentioned that curve c shows a shorter T_{max} than that of curve b although the polymerization current of the former is smaller than the latter. This phenomenon may be explained by the fact that the precipitation of the insoluble oligomer nuclei on the Au working electrode is not directly controlled by the applied polymerization current or potential.[43] We suggest that the T_{max} reflect a proportional

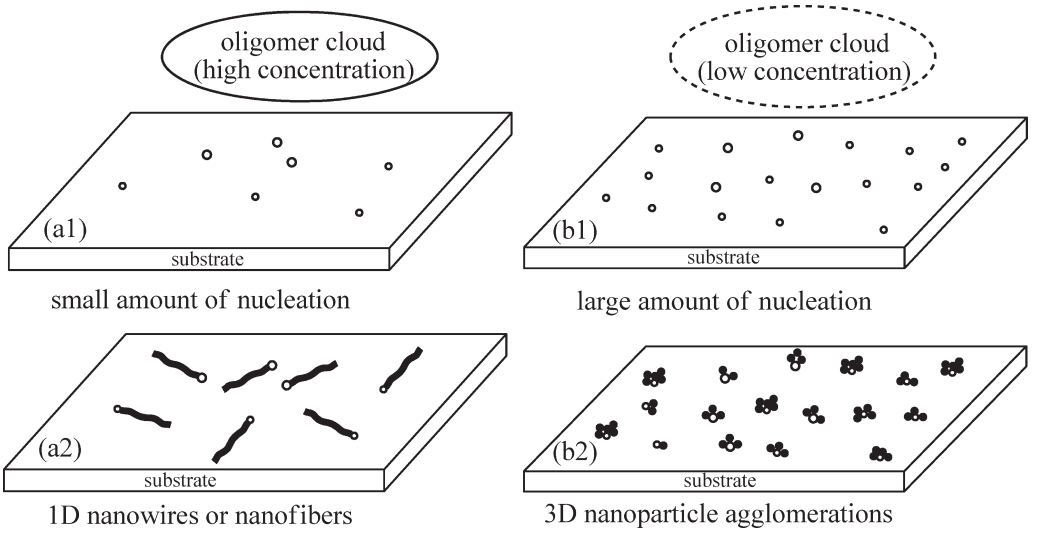

Figure 6. A mechanism proposed for the formation of two typical nanostructures under different polymerization conditions. (a) A high oligomer concentration and a small amount of nucleation on the substrate tend to give 1D nanowires or nanofibers. (b) A low oligomer concentration and a large amount of nucleation on the substrate tend to give 3D nanoparticle agglomerations.

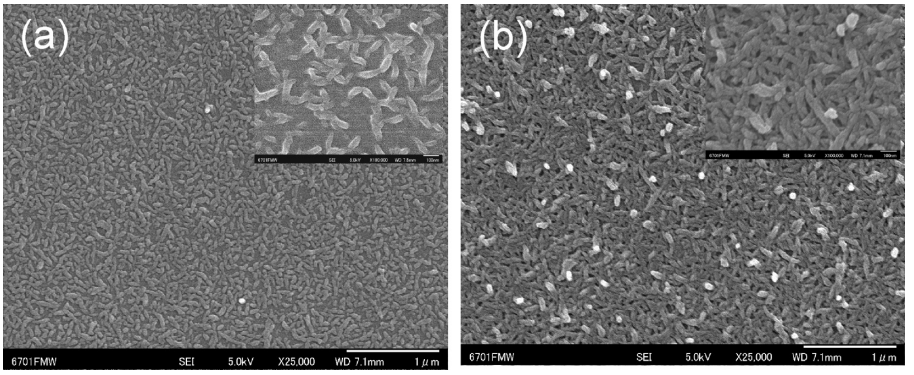

Figure 7. SEM images of nano-PANIs deposited on the APTES-treated electrodes with a current of 3 μA and a time of 1800 s (a) and 2700 s (b). The insets are the images with high magnification.

relation between the oligomer deposition and the oligomer diffusion occurred on the working electrode. Although the details of the relation are not clear yet, the value of T_{max} can be used to judge whether a polymerization is beneficial to producing a relatively high oligomer concentration on the insulating gap area.

The above experimental results demonstrate that two major factors, the oligomer concentration and the amount of nucleation, determine the morphology of PANI deposited on the solid substrates. On the basis of this finding, a deposition model is proposed to guide the preparation of conducting polymers with different nanostructures and orientations on solid substrates (Figure 6). In the case of a high oligomer concentration (especially a supersaturation state) and a small amount of nucleation, the deposition of oligomers may be dominated by the homogeneous nucleation process and thus tends to give nanostructures with horizontal orientation. However, in the case of a low oligomer concentration and a large amount of nucleation, the deposition may be dominated by the heterogeneous nucleation process and thus tends to form the nanoparticle agglomerations. The oligomer concentration can be regulated by parameters such as the monomer concentration or the polymerization current. The amount of nucleation can be regulated by parameters related to the interfacial energy, such as the hydrophilic/hydrophobic character or the surface roughness. It is noteworthy that the oligomer concentration and the nucleation amount can interact with each other during the polymerization. The fewer the nucleation on the substrates, the more the oligomers can be accumulated to create a high concentration environment. In contrast, the more the nucleation on the substrates, the faster the oligomers can be consumed to afford a low concentration environment. Thus, controlling the primary growth in the early stages is critical to the horizontal orientation because after that period the heterogeneous nucleation will result in a loss of the horizontal orientation.

For the application as chemiresistive gas sensors, the most ideal nanostructure across the gap area should be a horizontally oriented, monolayered, 2D nanofiber (or nanowire) conducting network. The deposition carried out on the highly hydrophilic substrate tends to give long nanofiers as shown in Figure 2a. However, it takes a relatively long time to form a conducting percolation network, which simultaneously increases the probability of the heterogeneous nucleation and growth. In order to seek a balance between the nucleation amount and the polymerization rate, a polymerization was tried on the APTES-treated electrodes with a current of 3 μA. Figure 7a indicates that the polymerization with a time of 1800 s affords an almost

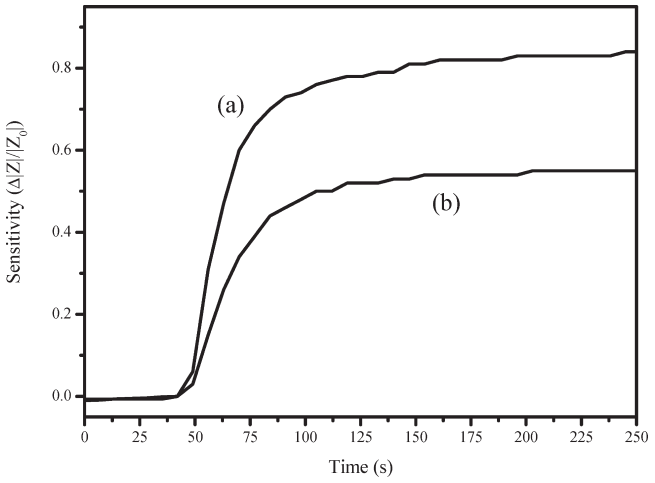

Figure 8. Real-time response of nano-PANI sensor devices upon exposure to 1 ppm ammonia gas. Curves a and b are corresponding to the films shown in Figures 7a and 7b, respectively.

monolayered nanowire network. The resistance of the fabricated electrode is ~2.4 kΩ, which verifies that a well-developed conducting percolation network is formed. With further growth to 2700 s, the monolayer film structure is replaced by a compact multilayer film structure. The perpendicularly oriented nanowires also tend to grow, which is characterized by the appearance of nodule-shaped white spots. We investigated the gas sensing character of the two electrodes upon exposure to ammonia gas with a concentration of 1 ppm. As shown in Figure 8, film a shows an obviously higher sensitivity than film b. Moreover, the response time of the former is also faster than the latter. The diffusion barrier caused by the film thickening may be one of the reasons for the sensitivity deterioration of film b. Additionally, we suggest that the quasi-1D conducting character of the percolation network is another important factor for the better sensing performance of film a because it can avoid the reduction of signal intensity caused by the lateral current shunting as usually observed in 2D films.[5]

CONCLUSION

In summary, a simple, template-free approach is developed to control the horizontally oriented growth of PANI nanowires or nanofibers on solid substrates. It is observed that the deposited morphology of PANI on the solid substrate is determined by the concentration of solution-formed oligomers and the nucleation amount of oligomers on the solid surface. Controlling deposition with high oligomer concentrations and limited nucleation amounts on the substrate surface is the key point to obtain 1D nanostructures with horizontal orientation. The gas sensing experiments confirm that the horizontal orientation helps to improve the sensing performance of the fabricated sensor devices. This method is simple and practical and thus has potential to be used in the fabrication of nanostructured conducting polymer chemiresistive sensors with high sensitivity but low cost.

AUTHOR INFORMATION

Corresponding Author

*E-mail liu@belab.ed.kyushu-u-ac.jp;Tel + 81-92-802-3729; Fax + 81-92-802-3770.

ACKNOWLEDGMENT

This work is supported by Regional Innovation Cluster Program (Global Type [second Stage]): R&D of bioelectronic technologies for safety and security and its application for sensing, from the Ministry of Education, Culture, Sport, Science and Technology, Japan.

REFERENCES

(1) Tran, H. D.; Li, D.; Kaner, R. B. *Adv. Mater.* **2009**, *21*, 1487–1499.
(2) Wan, M. *Adv. Mater.* **2008**, *20*, 2926–2932.
(3) Zhang, D.; Wang, Y. *Mater. Sci. Eng., B* **2006**, *134*, 9–19.
(4) Wan, M. *Macromol. Rapid Commun.* **2009**, *30*, 963–975.
(5) Wanekaya, A. K.; Chen, W.; Myung, N. V.; Mulchandani, A. *Electroanalysis* **2006**, *18*, 533–550.
(6) Bhadra, S.; Khastgir, D.; Singha, N. K.; Lee, J. H. *Prog. Polym. Sci.* **2009**, *34*, 783–810.
(7) Liang, L.; Liu, J.; Windisch, C. F.; Exarhos, G. J.; Lin, Y. *Angew. Chem., Int. Ed.* **2002**, *41*, 3665–3668.
(8) Pathasarathy, R. V.; Martin, C. R. *Nature* **1994**, *369*, 298–301.
(9) Parthasarathy, R. V.; Martin, C. R. *Chem. Mater.* **1994**, *6*, 1627–1632.
(10) Martin, C. R. *Chem. Mater.* **1996**, *8*, 1739–1746.
(11) Liu, J.; Lin, Y.; Liang, L.; Voigt, J. A.; Huber, D. L.; Tian, Z. R.; Coker, E.; Mckenzie, B.; Mcdermott, M. J. *Chem.—Eur. J.* **2003**, *9*, 604–611.
(12) Chiou, N.-R.; Lu, C.; Guan, J.; Lee, L. J.; Epstein, A. J. *Nature Nanotechnol.* **2007**, *2*, 354–357.
(13) Virji, S.; Huang, J.; Kaner, R. B.; Weiller, B. H. *Nano Lett.* **2004**, *4*, 491–496.
(14) Bartlett, P. N.; Ling-Chung, S. K. *Sens. Actuators* **1989**, *20*, 287–292.
(15) Reemts, J.; Parisi, J.; Schlettwein, D. *Thin Solid Films* **2004**, *466*, 320–325.
(16) Wang, J.; Chan, S.; Carlson, R. R.; Luo, Y.; Ge, G.; Rie, R. S.; Heath, J. R.; Tseng, H.-R. *Nano Lett.* **2004**, *4*, 1693–1697.
(17) Wang, J.; Bunimovich, Y. L.; Sui, G.; Savvas, S.; Wang, J.; Guo, Y.; Heath, J. R.; Tseng, H.-R. *Chem. Commun.* **2006**, 3075–3077.
(18) Shirsat, M. D.; Bangar, M. A.; Deshusses, M. A.; Myung, N. V.; Mulchandani, A. *Appl. Phys. Lett.* **2009**, *94*, 083502.
(19) Kemp, N. T.; Cochrane, J. W.; Newbury, R. *Nanotechnology* **2007**, *18*, 145610.
(20) Kemp, N. T.; Cochrane, J. W.; Newbury, R. *Synth. Met.* **2009**, *159*, 435–444.
(21) Ramanathan, K.; M. A. Bangar, M. A.; Yun, M.; Chen, W.; Mulchandani, A.; Myung, N. V. *Nano Lett.* **2004**, *4*, 1237–1239.
(22) Yun, M.; Myung, N. V.; Vasquez, R. P.; Lee, C.; Menke, E.; Penner, R. M. *Nano Lett.* **2004**, *4*, 419–422.
(23) Kemp, N. T.; McGrouther, D.; Cochrane, J. W.; Newbury, R. *Adv. Mater.* **2007**, *19*, 2634–2638.
(24) Thapa, P. S.; Yu, D. J.; Wicksted, J. P.; Hadwiger, J. A.; Barisci, J. N.; Baughman, R. H.; Flanders, B. N. *Appl. Phys. Lett.* **2009**, *94*, 033104.
(25) Nishizawa, M.; Shibuya, M.; Sawaguchi, T.; Matsue, T.; Uchida, I. *J. Phys. Chem.* **1991**, *95*, 9042–9044.
(26) Nishizawa, M.; Miwa, Y.; Matsue, T.; Uchida, I. *J. Electrochem. Soc.* **1993**, *140*, 1650–1655.
(27) Malinauskas, A. *Polymer* **2001**, *42*, 3957–3972.
(28) Sapurina, I.; Riede, A.; Stejskal, J. *Synth. Met.* **2001**, *123*, 503–507.
(29) Riede, A.; Helmstedt, M.; Sapurina, I.; Stejskal, J. *J. Colloid Interface Sci.* **2002**, *248*, 413–418.
(30) Sapurina, I.; Osadchev, A. Y.; Volchelk, B. Z.; Trchová, M.; Riede, A.; Stejskal, J. *Synth. Met.* **2002**, *129*, 29–37.
(31) Travain, S. A.; Souza, N. C.; Balogh, D. T.; Giacometti, J. A. *J. Colloid Interface Sci.* **2007**, *316*, 292–297.

(32) Stejskal, J.; Sapurina, I.; Trchova, M. *Prog. Polym. Sci.* **2010**, *35*, 1420–1481.
(33) Huang, J.; Kaner, R. B. *Angew. Chem., Int. Ed.* **2004**, *43*, 5817–5821.
(34) Tran, H. D.; Wang, Y.; D'Arcy, J. M.; Kaner, R. B. *ACS Nano* **2008**, *2*, 1841–1848.
(35) Li, D.; Kaner, R. B. *J. Am. Chem. Soc.* **2006**, *128*, 968–975.
(36) Li, D.; Huang, J.; Kaner, R. B. *Acc. Chem. Res.* **2009**, *42*, 135–145.
(37) Bunker, B. C.; Rieke, P. C.; Tarasevich, B. J.; Campbell, A. A.; Fryxell, G. E.; Graff, G. L.; Song, L.; Liu, J.; Virden, J. W. *Science* **1994**, *264*, 48–55.
(38) Sasaki, K.; Kaya, M.; Yano, J.; Kitani, A.; Kunai, A. *J. Electroanal. Chem.* **1986**, *215*, 401–407.
(39) Liu, C.; Hayashi, K.; Toko, K. *Electrochem. Commun.* **2010**, *12*, 36–39.
(40) Liu, C.; Hayashi, K.; Toko, K. *Synth. Met.* **2009**, *159*, 1077–1081.
(41) Bade, K.; Tsakova, V.; Schultze, J. W. *Electrochim. Acta* **1992**, *37*, 2255–2261.
(42) Córdova, R.; Valle, M. A.; Arratia, A.; Gómez, H.; Schreber, R. *J. Electroanal. Chem.* **1994**, *377*, 75–83.
(43) Komsiyska, L.; Tsakova, V.; Staikov, G. *Appl. Phys. A: Mater. Sci. Process.* **2007**, *87*, 405–409.